Energy Balance Climate Models: Stability Experiments with a Refined Albedo and Updated Coefficients for Infrared Emission

J. OERLEMANS AND H. M. VAN DEN DOOL

Royal Netherlands Meteorological Institute, De Bilt, The Netherlands

(Manuscript received 7 September 1977, in final form 22 November 1977)

ABSTRACT

A zonally averaged climate model of the energy-balance type is examined. Recently published satellite measurements were used to improve existing parameterizations of planetary albedo and outgoing radiation in terms of surface and sea level temperature. A realistic constant for the diffusion of energy was found by tuning the model to the present climate. For the actual solar constant both the present climate and an ice-covered earth are solutions of the model. They are extremely stable for temperature perturbations.

The effect of variation of the solar constant was investigated in detail. If the solar constant is decreased by 9–10% the warm solution (partial ice cover) jumps to the cold one (complete ice cover). Transition from the cold to the warm solution requires an increase of the solar constant to 109–110% of its present value. Therefore, we conclude that the model climate is much more stable with regard to variations in the solar input than has been assumed so far. This is caused mainly by our updated formulation of the outgoing radiation. Further experiments showed that our model is much more sensitive to changes in the outgoing radiation than to changes in the diffusivity for energy.

1. Introduction

During the last decade the increasing demand for knowledge of climate and climatic variations has led to the establishment of an extensive hierarchy of climate models. At the base of this hierarchy are the well-known energy-balance models (EBM's). Most models of this kind are based on a zonally, vertically and time-averaged balance of incoming and outgoing radiation and divergence of the energy transport in atmosphere and ocean. It is assumed *a priori* that the conservation laws for mass and momentum are satisfied. Budyko (1969) and Sellers (1969) were the first to construct an EBM and they arrived at alarming results: a drop of 2% of the solar constant or a 3% increase in the atmosphere's infrared transmissivity would lead to a completely ice-covered earth.

Since that time many investigators have carried out experiments with EBM's. Schneider and Gal-Chen (1973) made the extension to a time-dependent model and Sellers (1976) developed a longitude-dependent model based on the energy-balance principle. Recently, much attention has been paid to an analytical approach, in order to obtain stability criteria and the number of possible solutions (e.g., North, 1975a,b; Chýlek and Coakley, 1975; Su and Hsieh, 1976; Frederiksen, 1976; Ghil, 1976). In broad outline these studies confirm the results of Budyko and Sellers.

The parameterization of albedo and outgoing radiation have received less attention. Cess (1976) discussed various feedback mechanisms and employed recent satellite measurements to estimate their effects. Lian and Cess (1977) explored the dependence of albedo on zenith angle and cloudiness. They derived expressions for the albedo and outgoing radiation and used them in the Budyko model. This brought to light the fact that the ice-albedo feedback had been overestimated. In this paper we will derive parameterizations of the albedo and outgoing radiation in a somewhat different way, but fully based on recent satellite measurements. We tried to do this without the aid of arbitrary fitting functions or consistency factors that are often used to fit the present climate. We feel that the use of such functions reduces the universality of the parameterizations.

Before going into the description of the model it is useful to obtain some insight into the difficulties involved if one studies the earth's climate with an EBM. The suitability of an energy-balance principle to model climate has not yet been shown definitely. The principal question is to what extent the components of the (zonally averaged) energy balance are affected by the dynamics of the climatic regime. This question is directly related to the possibility of expressing quantities that constitute the energy balance in a single variable, namely, the temperature at a fixed level. There are two major ways in which the large-scale circulation affects the energy balance. First, there is the distribution of cloud cover over the globe which is closely related to the stream pattern. The cloudiness affects the radiation balance by

0022-4928/78/0371-0381$05.50

lowering the radiation temperature and reflecting incoming solar radiation. Second, the atmosphere's capacity for transporting energy to regions with a negative radiation balance depends on the strength of the Hadley cell, the mid-latitude eddies, etc. Moreover, energy-transporting ocean currents are mainly driven by wind stress. However, these facts do not imply that it is necessary to compute the circulation explicitly: it probably is sufficient to use a proper parameterization of the energy transport. Gal-Chen and Schneider (1976) carried out experiments with various formulations of the energy transport and arrived at the conclusion that the parameterizations of the planetary albedo and outgoing radiation are far more important than that of the energy transport.

The relation between the general circulation and cloudiness and cloud height is a more serious problem. It seems to be impossible to construct a functional relationship between a fixed-level temperature and cloudiness. To our knowledge, even the direction of change in cloudiness due to a rising surface temperature is very uncertain. With regard to the lapse rate the same difficulties arise. This leaves only one realistic approach: to ignore variations in cloudiness and lapse rate. Some support to this approach may be found in a study by Gates (1976), who simulated the ice-age climate with a general circulation model. His results show that global cloudiness during the last ice age hardly differed from today's. In addition, Cess (1976) presents evidence indicating that cloudiness does not act as an important feedback mechanism. In contrast to these findings, Temkin and Snell (1976) state that cloudiness acts as a negative feedback mechanism, i.e., it stabilizes the earth's climate.

2. The model

In the present model the sea level temperature is used as the principal dependent variable. The steady-state formulation of the vertically and zonally averaged energy balance for any latitude φ may be written

$$D\nabla^2 T+Q(1-\alpha)=I, \tag{1}$$

where:

T sea-level temperature
Q incoming solar radiation
α effective planetary albedo
I infrared radiation emitted to space
D diffusivity for total energy

∇^2 Laplace operator $\left[=\dfrac{\partial^2}{\partial\varphi^2}-\tan\varphi\dfrac{\partial}{\partial\varphi}\right]$.

A factor equal to the square of the earth's radius which should appear in the Laplace operator is absorbed in D. In (1) the first term represents the divergence of the energy transport and the second term is the net solar radiation gained by the column. The right-hand side of (1) denotes the energy sink of the system, namely, the infrared emission to space.

In regions that are snow-covered during a part of the year there exists a coupling between incoming radiation and albedo. In oceanic regions the relation between the sun's elevation and the fraction of incoming radiation reflected back to space also contributes to this coupling. Larger amounts of incoming radiation are connected with lower albedos, so the use of the real mean planetary albedo would lead to an underestimation of the incoming energy. Therefore, we use in (1) the albedo derived from the *annual mean* radiation balance and call it the *effective* planetary albedo. The difference between the mean and effective albedo as computed from the data given by Ellis and Vonder Haar (1976) appeared to be small: we found maximum values of a few percent around 60° latitude.

The divergence term in (1) needs some motivation. We based it on the feeling that the numerous feedback mechanisms in the ocean and atmosphere suppress the effect of favorable conditions for a specific energy-transporting system on the total energy transport. An example of feedback acting in this way was found by Manabe and Terpstra (1974). Their experiments with the GFDL general circulation model brought to light that the contribution of the transient eddies to the energy transport adjusts itself to that of the orographically forced stationary waves. Omission of the forcing by mountains showed that the transient eddies transport more energy in that case, *keeping the total energy transport at approximately the same rate.* Therefore, a simple formulation is likely to be as good as (or even better than) a parameterization that uses various circulation subdivisions such as transient eddies, stationary eddies, mean circulation cells, etc. We decided to use a formulation that is diffusive with respect to T. This choice is in accordance with the results of Gal-Chen and Schneider (1976) who state that a diffusive form is probably the most suitable one.

3. Parameterization of the outgoing radiation

For some time the infrared emission to space has been estimated by methods like that of Elsaesser (e.g. Sellers, 1965). The poorly known distribution of water vapor in the atmosphere is a major source of errors in such methods. However, a standard set of satellite measurements concerning the radiation balance of the earth-atmosphere system has been presented recently by Ellis and Vonder Haar (1976). Since these measurements were taken at the top of the atmosphere, they should provide an excellent base for the parameterization of both the infrared emission and the albedo.

Fig. 1a shows the observed values of the annual infrared emission and the corresponding observed mean sea level temperatures for 10° latitude belts. Relation (a) has been used by North (1975a) and is a linearized version of Sellers' parameterization that was also used by Schneider and Gal-Chen (1973). Frederiksen (1976) and North (1975b) applied parameterization (b) to their models. Fig. 1a shows that the variation of infrared emission with temperature has been underestimated. To simulate the present climate this has often been compensated by adjustment of other parameters (such as the diffusivity for energy), but we will show that *the stability of the earth's climate is much greater if the infrared parameterization as suggested by the satellite data of Ellis and Vonder Haar is used.* This parameterization is shown in Fig. 1b. Instead of the sea level temperature we used the mean surface temperature T_s, which gave a better fit (compare the scatter in Fig. 1a with that in Fig. 1b). The formulation of the infrared emission applied in the model is given by

$$I = I_0 + b(T - h\Gamma), \tag{2}$$

where in the standard case $I_0 = 205$ W m^{-2} and $b = 2.23$ W (m^2 °C)$^{-1}$. Here, Γ is the lapse rate (6°C km^{-1}) and h the zonal mean height of the surface. Our value of b is larger than the one obtained by Cess (1976), who used the same satellite data. He arrived at $b = 1.6$ W (m^2 °C)$^{-1}$ due to the use of lower temperatures at the poles. Held and Suarez (1974) have recommended using the temperature at 500 mb based on data concerning the *seasonal* variation of I. Cess (1976) showed that $\partial I/\partial T$ derived from the seasonal variation of I can be twice as much as that derived from the variation of the annual emission with latitude. Consequently, it is not obvious that the result of Held and Suarez holds for annual mean conditions.

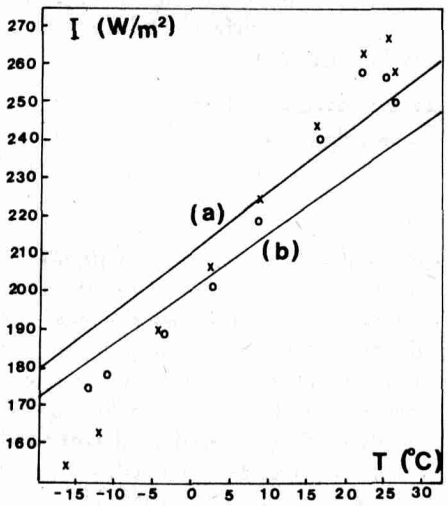

FIG. 1a. The annual infrared emission as a function of the mean sea level temperature for belts of 10° latitude. Circles refer to the Northern Hemisphere, crosses to the Southern. Lines (a) and (b) indicate relations used by earlier workers.

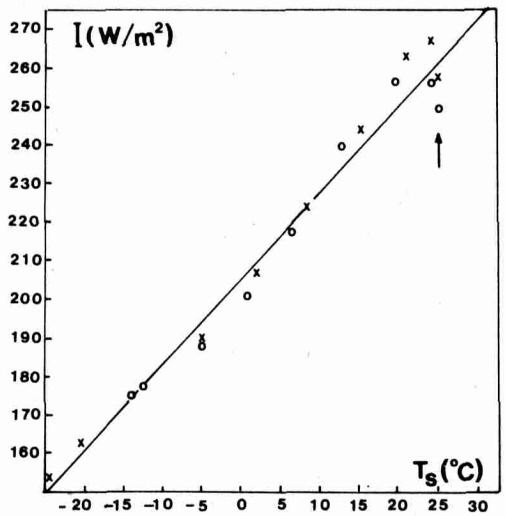

FIG. 1b. As in Fig. 1a except for the surface temperature. The straight line shows the parameterization used in the model. The arrow indicates the dip in I in the equatorial region.

Fig. 1b shows that for temperatures around 25°C a dip in the outgoing radiation occurs. Since these temperatures correspond to the equatorial region, the dip is probably associated with the cloudiness in the ITCZ. Eq. (2) does not represent the dip, but the neglect of the ITCZ clouds in the simulation of the albedo (to be disdussed in the next section) leads to a small overestimate of the incoming energy which counteracts the error caused by the omission of the dip in I. In any event, the small deviation of the observed values of I from the linear approximation given by (2) gives confidence.

4. Parameterization of the albedo

Since it determines to a large extent the number of solutions of an EBM (e.g., Frederiksen, 1976), we paid special attention to the albedo. We based the final albedo $\alpha(\varphi)$ on a set of planetary albedos associated with different conditions at the surface. These conditions are derived following the scheme given in Fig. 2. The surface temperature, averaged over the *continental* part of the belt considered (denoted by T_1) is computed along with the constant lapse rate Γ. Sea and land are treated separately using T and T_1, respectively. The ice-covered fraction of the sea surface is given by

$$\Delta_{tics} = \begin{cases} 1, & T < -20°\text{C} \\ 0.5 - \arctan[(T+10)/2]/\pi, & -20 < T < 0°\text{C} \\ 0, & T > 0°\text{C}. \end{cases} \tag{3}$$

The ice cover on land (Δ_{ticl}) is also computed with (3), using T_1 instead of T. Eq. (3) is a somewhat smoothed version of the most often used boundary of the ice

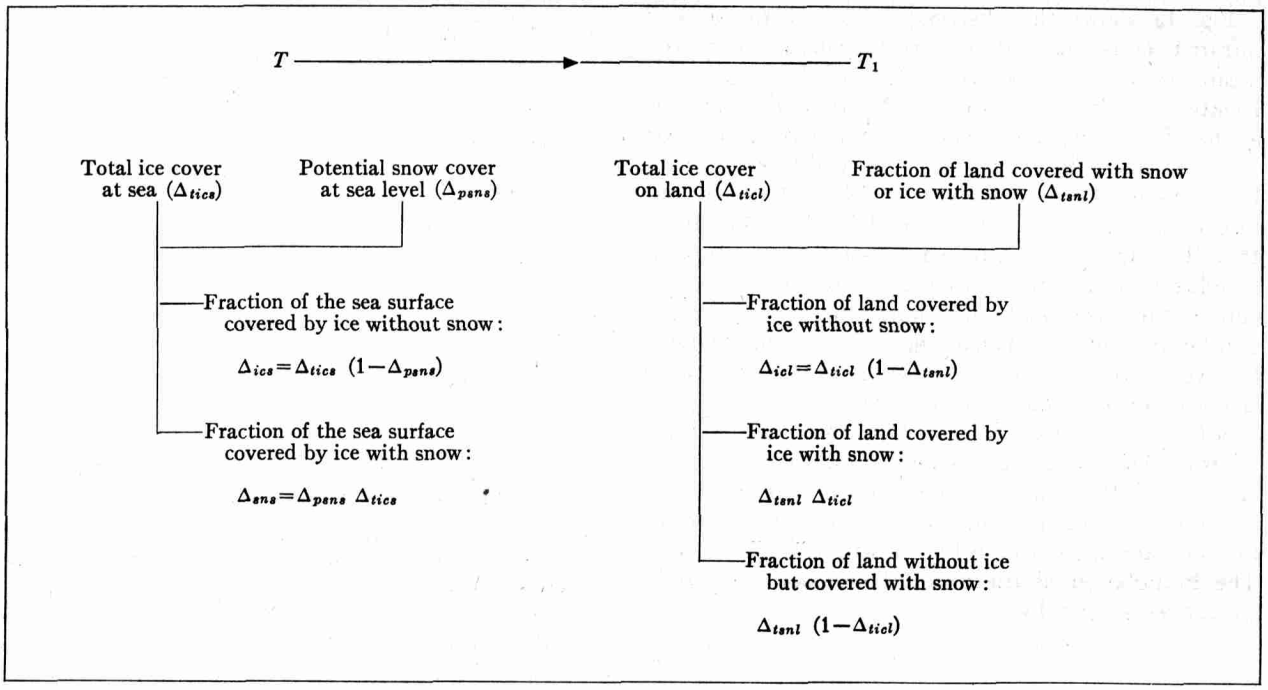

FIG. 2. Scheme for the computation of ice and snow cover in oceanic and continental regions, starting from the sea level temperature T.

cover, namely, $T=-10$°C. This smoothing has been applied since the edge of the ice cap or the sea ice may be expected to vary considerably with longitude as suggested by the results of CLIMAP (1976). The potential snow cover, i.e., the snow cover that would exist if open water did not melt the falling snow, can be derived from observations taken at climatological stations that are distributed uniformly over the Northern Hemisphere. Fig. 3 gives a plot of annual mean temperature as a function of the number of days with snow cover. The data were taken from Lamb (1972). There appears to be a rather strong correlation, which is represented in the model by

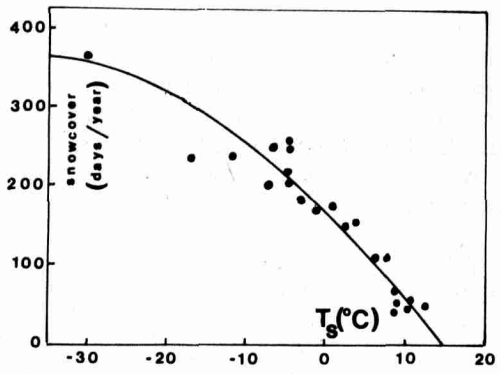

FIG. 3. The number of days with snow cover as a function of the mean annual temperature (data from Lamb, 1972). The curve gives the parameterization used in the model.

$$\text{snow cover} = \begin{cases} 1, & T<-40\text{°C} \\ 1-0.00033(T+40)^2, & -40<T<15\text{°C} \\ 0, & T>15\text{°C}. \end{cases} \quad (4)$$

To get Δ_{psns} and Δ_{tsnl} (see Fig. 2), T and T_1 are used, respectively.

Following the scheme in Fig. 2 and introducing albedos for the various surface conditions the planetary albedo may be written

$$\alpha(\varphi)=[\Delta_{ics}\alpha_{ic}+\Delta_{sns}\alpha_{sn}+(1-\Delta_{ics}-\Delta_{sns})\alpha_{se}](1-\Delta) +[\Delta_{icl}\alpha_{ic}+\Delta_{ticl}\Delta_{tsnl}\alpha_{sn}+\Delta_{tsnl}(1-\Delta_{ticl})\alpha^*_{sn} +(1-\Delta_{icl}-\Delta_{tsnl})\alpha_{la}]\Delta, \quad (5)$$

where:

α_{ic} albedo over an ice-covered area (0.56)
α_{sn} albedo over a snow-covered area (0.61)
α_{la} albedo over land without ice or snow (0.31)
α_{se} albedo over the ocean; the φ-dependence represents the influence of the sun's mean elevation $[=0.337-0.125\cos(2\varphi)+0.007\exp(\varphi^2)]$
α^*_{sn} albedo over snow-covered land corrected for the presence of trees as discussed below
Δ fraction of land along a latitude circle.

We estimated the various albedos from charts published by Raschke *et al.* (1973). Since the albedo over snow-covered regions is overestimated if exten-

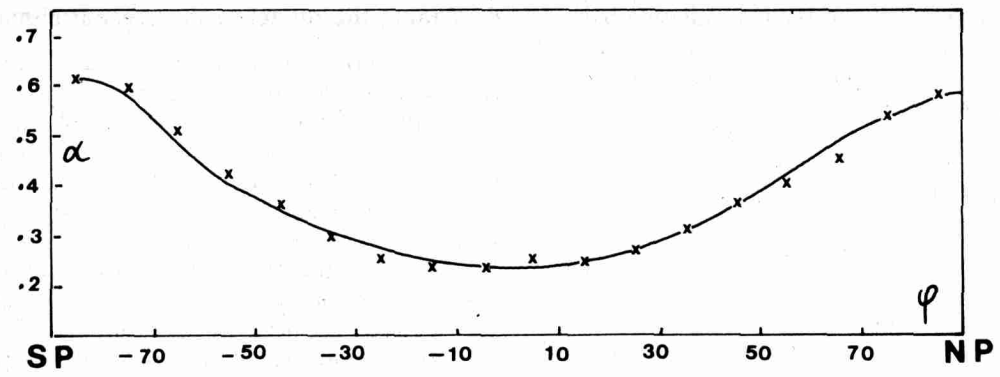

FIG. 4. Computed albedo (solid line) compared with observed values given by Ellis and Vonder Haar (1976).

sive forests are present we made a correction by introducing a woody zone. This zone is centered at $T=7.5$°C with a cover of 50%, gradually becoming 0% for $T=-2.5$°C and 25% for $T=15$°C (for higher values of T the snow cover vanishes completely). The albedo of snow-covered forest has been set at 0.41.

So far we constructed the parameterization of the albedo without adjustments by means of arbitrary φ-dependent factors in order to match the observed values. For the sake of generality such factors should be avoided if possible. Fig. 4 shows the computed albedo corresponding to the present temperature distribution. Values observed by satellites are indicated with crosses (Ellis and Vonder Haar, 1976). Although variation of cloudiness has not been taken into account, the computed albedo distribution resembles the observed one surprisingly well. At all latitudes the computed values lie within the range of uncertainty of the observations. We conclude that there is no reason to introduce a φ-dependent correction factor for one or more of the albedos used.

It is interesting to see how the planetary albedo depends on temperature at various latitudes. Fig. 5 shows α isopleths in a φ, T diagram, computed following (5). Everywhere the albedo decreases with increasing temperature but the rate of decrease varies widely with latitude. The sharp angle of the isopleths near -7°C and 70°S is caused by the transition from 100% continent to 100% ocean (the edge of Antarctica). Another feature is the very smooth decrease of albedo with increasing temperature in the mid-latitudes of the Northern Hemisphere; this effect is due to a large fraction of land permitting extensive snow cover. Fig. 5 clearly shows that there are significant asymmetries with respect to the equator, caused entirely by differences in the fraction of land and mean elevation.

5. Method of solution

Eq. (1) is solved numerically by an iterative method. For the present goal a discretization on 36 points gives sufficient resolution; these points are defined by $\varphi_i=-87.5+5(i-1)$, with $i=1,\ldots,36$. Negative values of φ refer to the Southern Hemisphere, positive values to the Northern Hemisphere. Since energy is not allowed to flow through the boundaries of the model, the condition $\partial T/\partial\varphi=0$ at the poles should be satisfied [for a discussion of boundary conditions in zonally averaged models see Hantel (1974)]. This is done by introducing two points at $\varphi=-92.5$° and 92.5° at which the sea-level temperature is set equal to $T(\varphi_1)$ and $T(\varphi_{36})$, respectively. Applying centered differences to the Laplace operator leads to the following formulation of the model

$$\mathbf{AT}=\mathbf{f}(\mathbf{T}), \tag{6}$$

where $\mathbf{A}$ is the matrix

$$\begin{pmatrix} -a_1-b & a_1 & & & \varnothing \\ a_{35} & c-b & a_2 & & \\ & a_{34} & \bullet & & \\ & & \bullet & \bullet & \\ & & & \bullet & a_{34} \\ & & & a_2 & c-b \quad a_{35} \\ & \varnothing & & & a_1 \quad -a_1-b \end{pmatrix},$$

with $a_i=1/d^2+(\tan\varphi_i)/2d$, $c=-2/d^2$, $d=5$° (grid distance). In (6), $\mathbf{T}$ is a vector with elements $T(\varphi_i)$

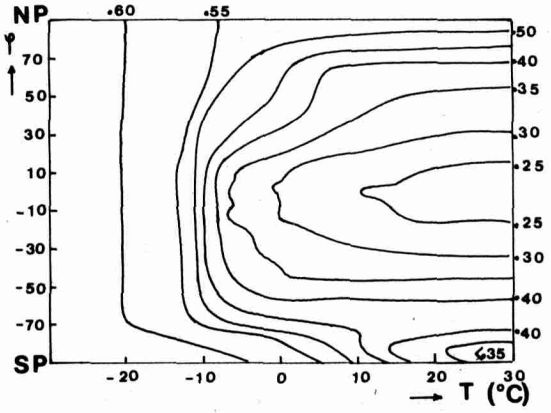

FIG. 5. The behavior of α as represented in the model. The albedo is shown as a function of sea level temperature and latitude.

and **f** is a vector consisting of the net radiation balance at the various grid points minus the part of I that varies linearly with T. This part, denoted by the proportionality constant b, is included in **A**. Such a procedure is necessary since otherwise **A** would be singular and could not be inverted.

Eq. (6) is solved by means of the iterative scheme

$$\mathbf{T}_{n+1}=\mathbf{A}^{-1}\mathbf{f}(\mathbf{T}_n). \tag{7}$$

This simple scheme appeared to be stable for all of our experiments and the convergence to solutions was fairly rapid. The iteration was ended if the condition $|T_{n+1}(\varphi_i)-T_n(\varphi_i)|<10^{-3}$ °C was satisfied for all i.

The mathematical aspects of analyzing the stability of EBM's have been discussed in detail by Held and Suarez (1974) and Ghil (1976). Here the following remarks will be sufficient.

Although we used a steady-state formulation, the stability properties of the solutions with respect to time may be investigated with the same method. If a term $C\partial T/\partial t$ is added to (1), where C is a time scale of the thermal inertia of the earth-atmosphere system, the resulting equation can also be solved by (7)—the scheme becomes implicit in that case. Successive steps are equivalent with points in time, the corresponding time step being equal to C. Since f satisfies a Lipschitz condition it can be shown that the asymptotic solution of a *stable* explicit scheme for the time-dependent case is the same as the one obtained by applying (7) for *any* initial field. These facts mean that stability experiments may be made by varying the first guess with which scheme (7) is started; in other words, *the concepts of first guess and initial conditions are completely equivalent*. It should be emphasized that (7) cannot produce unstable solutions. Since such solutions will not appear in nature they have no practical significance. In the following sections the word solution should be interpreted as a model climate that is stable with regard to sufficiently small perturbations of **T**.

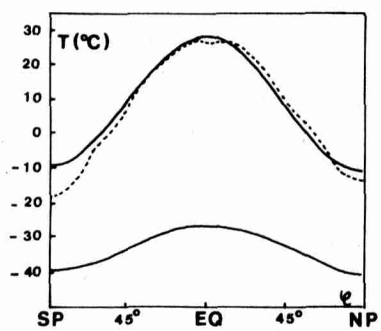

FIG. 6. Sea level temperature of the two solutions for the present value of the solar constant (solid lines) and the observed sea level temperature (dashed line).

6. Tuning the model to the present climate

A procedure often applied to tune an EBM to present conditions is that of varying the constant(s) in the formulation of the energy transport. We also followed this approach and obtained a best fit to the observed temperature distribution if D was set at 0.70 W (m² °C)$^{-1}$. Starting with cold initial conditions another solution was found: the completely ice-covered earth. Fig. 6 shows the two steady-state solutions for the present solar constant S_0 (1365 W m^{-2}) together with the observed sea level temperature distribution. The simulated temperature field is good except at high latitudes in the Southern Hemisphere. This is due to the fact that points $\varphi<-60°$ were ignored in determining the value of D that gives the best fit. The main reason for such a procedure was the expected uncertainty of the "observed sea level temperature" over Antarctica, due to the necessary choice of an arbitrary lapse rate. However, the observed temperature difference between the arctic and antarctic regions decreases rapidly with height indicating that the computed T (which has to be representative of the whole atmospheric column!) should be higher than "observed" in the antarctic region. It should be noted, in contrast to the models of Faegre (1972) and Frederiksen (1976), that our model never produced an ice-free solution. Even with a stepfunction for the albedo (Budyko, 1969) such a solution did not show up.

The optimum value of D for the present model [0.70 W (m² °C)$^{-1}$] is in good agreement with a recent estimate of the total energy balance made by Oort and Vonder Haar (1976). Based on their data we derived a linear regression of the poleward energy transport and the sea level temperature gradient, suggesting that $D=0.62$ W (m² °C)$^{-1}$. In view of the model's insensitivity to changes in D (this will be discussed in Section 8), the difference between the observed and "tuned value" of D is of no significance.

The evolution of the climate for different initial conditions was investigated by varying the first guess according to

$$T_0(\varphi_i)=p+q\cos(2\varphi_i). \tag{8}$$

This guess has two degrees of freedom and is always symmetric with respect to the equator; p is the temperature at 45° and q is half the equator-to-pole temperature difference. Since any initial field converges to one of the solutions mentioned above, the p,q plane can be divided into two distinct regions in which convergence to the same asymptotic solution occurs as shown in Fig. 7. The solid line can be interpreted as an unstable neutral limit line; the model climate never crosses this line. The limit line also reflects the existence of an intermediate unstable solution (e.g., North, 1975b; Ghil, 1976).

In order to simplify the explanation of Fig. 7 we take $q=0$, i.e., a constant temperature over the globe

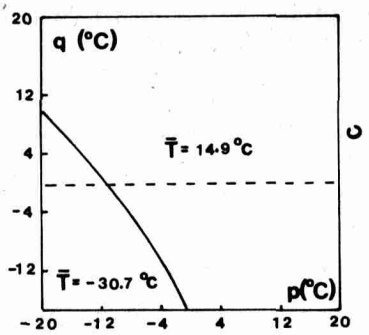

FIG. 7. The two regions of initial conditions, separated by the solid line, with the global mean temperature of the corresponding asymptotic solutions.

as a first guess (indicated by the dashed line). For $T_0 < -12°C$ the asymptotic solution is an ice-covered earth, whereas for $T_0 > -12°C$ the present climate is the final solution. Since the global mean initial temperature is given by $\bar{T}_0 = p + q/3$, isopleths of $\bar{T}_0$ in Fig. 7 will have a slope $\partial q/\partial p = -3$. It is easy to see that, regardless of the initial temperature difference between pole and equator, the climate always returns to the warm equilibrium solution if the global mean initial temperature is at least $-6°C$. Apparently, at the moment we are far from conditions that would lead to an ice-covered earth. We conclude that the model climate is very stable with regard to perturbations in the temperature field.[1]

With the present resolution of the model (36 grid points) it is possible to investigate the stability properties with 36 degrees of freedom instead of two as discussed above. However, small-scale features are damped more quickly by the diffusion of energy (North, 1975a), so they are probably less important in the evolution of the model climate. Furthermore, the practical significance of starting with "wild" initial conditions is not clear, so we did not carry out a more general stability analysis.

7. Sensitivity to changes in the solar constant

A comparison of several studies with EBM's makes clear that these models may simulate the present zonal mean temperature distribution for a certain range of infrared emission coefficients (b in this study) by adjustment of the transport constant(s) for energy. But what happens if the solar constant changes? It may very well be that the behavior of the model with other solar inputs depends to a high degree on the particular choice of b. As will be shown in Section 8 this turns out to be the case. In the following S denotes the solar constant normalized by its present value. A bar indicates a global mean.

Extensive numerical experiments with a set of initial conditions for a range of values of S led to the picture given in Fig. 8 where the global mean temperature is shown as a function of S. The solution diagram shows two branches, one corresponding to the warm climate, the other to the cold one. The present climate is indicated by a circle. Starting with today's climate decreasing S results in a climate that gradually becomes cooler until, for $S = 0.905$, the solution jumps spontaneously to the cold branch, corresponding to the completely ice-covered earth. A further decrease of S still lowers $\bar{T}$. It would not be easy to come back to the present climate: even

[1] When writing this article we became aware of an Abstract by T. H. Vonder Haar and J. S. Ellis (Abstracts of papers presented at the XVI General Assembly of the UGGI, Grenoble, 1975) which stated that parameterizations based on satellite data indicate that the global climate is more stable. To our knowledge, no paper in which their experiments and results are discussed has been published in a current journal.

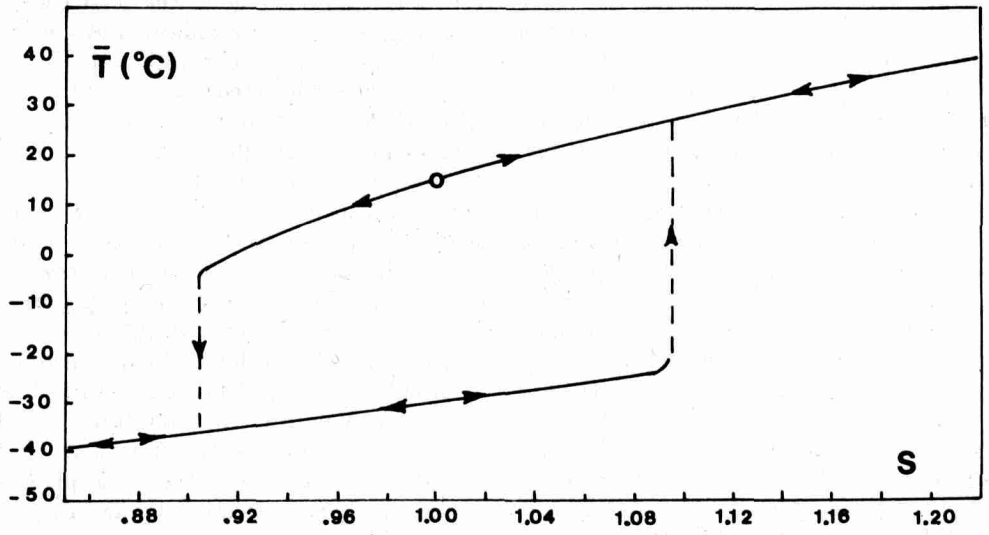

FIG. 8. Solutions of the model, represented by means of the global mean temperature, for a wide range of solar constants.

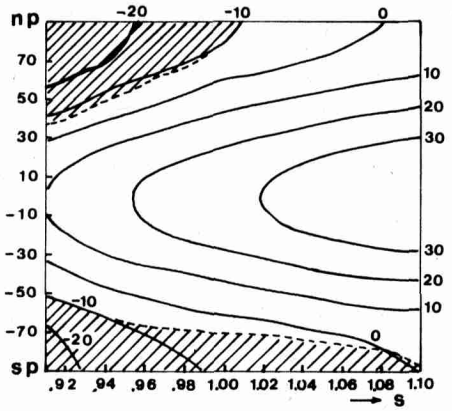

FIG. 9. Sea level temperature distribution in the warm branch for a range of solar constants. Isotherms are drawn every 10°C; hatched areas indicate an ice cover of 50% or more.

for $S=1.05$ a temperature perturbation of 12°C would be required to jump to the warm branch again. If S reaches 1.095 this jump goes spontaneously and the cold branch disappears. The points where the jump from one branch to the other one occurs are called transition points. Except in the very neighborhood of these transition points, the solutions are stable for realistic temperature perturbations (say a few degrees). This makes it possible to draw arrows in the diagram, according to which the solution moves if S is varied.

The diagram has a remarkably regular shape. The present climate is situated on the warm branch just halfway between the transition points. Both the warm and the cold branches resemble straight lines, which can be explained easily. Integrating (1) with respect to φ yields the global energy balance

$$I_0+b\bar{T}=\overline{Q(1-\alpha)}=\tfrac{1}{4}S_0S(1-\bar{\alpha})-\overline{\alpha'Q'}. \qquad (9)$$

If the correlation between α and Q over the globe is independent of S, a graph of $\bar{T}$ vs S will show a straight line with slope $S_0(1-\bar{\alpha})/4b$. In the cold branch (larger $\bar{\alpha}$) the slope is therefore smaller than in the warm branch (smaller $\bar{\alpha}$). The formal expression for the slope should be kept in mind for the discussion in Section 8.

The latitudinal distribution of the sea level temperature for the warm branch is shown in Fig. 9. For some solar constant (horizontal axis) the corresponding climate is represented by a line going upward. Latitudes with an ice cover of 50% or more are hatched. There are some notable differences between the Northern and Southern Hemispheres. For low values of S the ice-covered area in the Northern Hemisphere is larger than in the Southern, but with increasing S the arctic ice sheet disappears much more rapidly than the antarctic. For a 1% increase of S, in the Northern Hemisphere the 50% ice-cover line disappears completely! The relatively high antarctic sea level temperatures that occur for small values of S are due to lower *surface* temperatures in that region resulting in a less intense emission of infrared radiation. For higher values of S this effect is obscured by the different properties of the surface in the southern and northern polar regions. At lower latitudes the picture shows very smooth isotherms and is fairly symmetric with respect to the equator.

8. Sensitivity to changes in empirical constants

Before discussing the significance of the results presented in Section 7 it is desirable to look at the sensitivity of the solution diagram to changes in the diffusivity and the formulation of the outgoing radiation.

Fig. 10 shows the solution diagram for three values of b with an adjustment of I_0 (the constant part of I) in order to keep the global mean outgoing radiation within reasonable bounds. Clearly, the picture shifts to the right for smaller values of b. The slope of the warm branch becomes steeper, in particular to the left of the present climate. For $b=1.75$, a 4% reduction of the solar constant results in a spontaneous transition to the ice-covered earth. However, the two-branch structure of the solution diagram does not change if b is varied within a realistic range.

In Fig. 11 the solution diagram for three different values of D is presented. It turns out that D affects the position of the transition points but the cold and warm branches almost coincide. A comparison of Figs. 10 and 11 makes clear that the stability properties are more sensitive to changes in the outgoing radiation than to changes in the diffusivity. This confirms the results of Gal-Chen and Schneider (1976).

9. Discussion

The most interesting feature of EBM's is the result that a certain decrease of the solar constant will lead to a completely ice-covered earth. According to Budyko (1969) this would occur with a 1.6% decrease. This alarming result inspired many scientists to experiment with EBM's and they arrived at similar results: a drop in S of roughly 2% initiates a climate with total ice cover. Comparing this to our results leaves only one conclusion: *our model climate is much more stable.* We found that for realistic temperature perturbations an *8–9% decrease of S seems to be required to cause the breakdown to the deep freeze.* Associated with the much larger critical decrease of S is the smaller change of $\bar{T}$ for a 1% decrease in solar input; in other words, the slope of the warm branch appears to be less. Values in the literature range from -5 to -3°C per 1% but we found a value of only -1.5°C per 1%. Recalling that the slope of $\bar{T}$ with respect to S can be approximated by $(1-\bar{\alpha})/(4b)$ it is clear that this can only be caused by the much larger value of b used in our model.

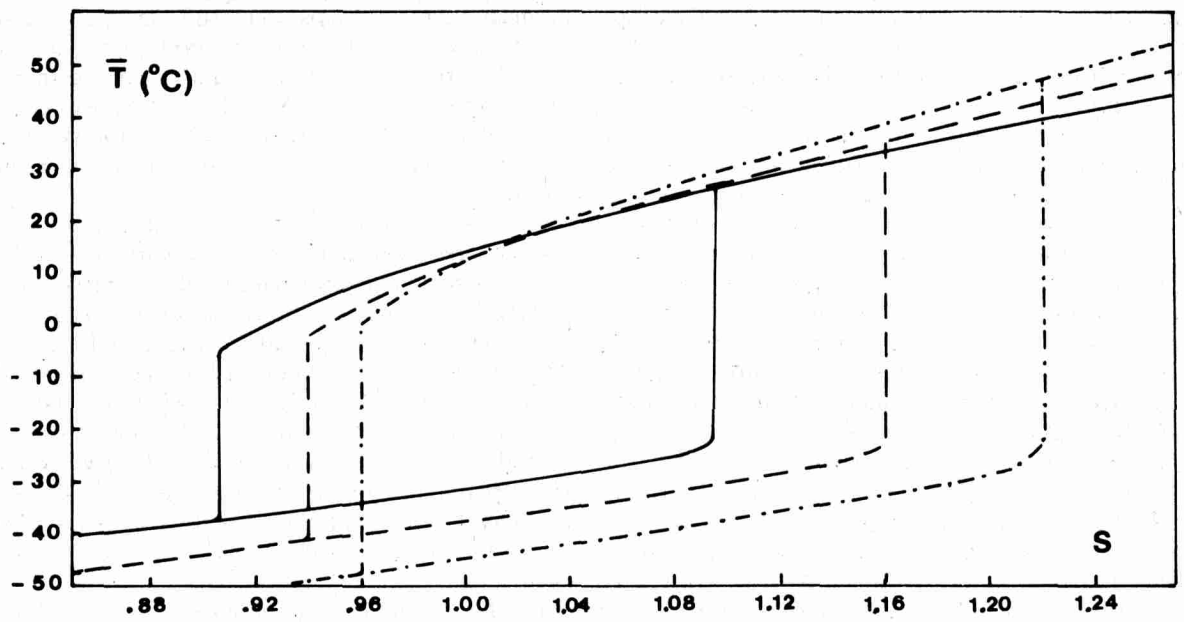

FIG. 10. Solution diagrams for three parameterizations of the outgoing radiation: $205+2.23\ T_s$ (solid line), $210+2.00\ T_s$ (dashed line), $213+1.75\ T_s$ (dot-dashed line) W m^{-2}. The solid line corresponds to the standard case.

Inspecting Fig. 10 again, it becomes clear why the present model gives different results. A decrease of b results in a steepening of the warm branch while the transition points move to the right. For $b=1.75$ W (°C m^2)$^{-1}$ the critical drop in solar input is only 4%. Since the values of b used in previous studies lie around 1.50 W (°C m^2)$^{-1}$ (see Fig. 1a), it is clear why a critical decrease of S of about 2% was found. From Fig. 11 it follows that the use of a different value for D could not neutralize this effect. *Therefore, the different results of the present model are almost completely due to a stronger coupling between surface temperature and outgoing radiation.* This may be understood as follows. A stronger coupling of temperature with outgoing radiation allows the net radiation balance to change little for a relative wide range of S because a small temperature change is enough to reestablish the balance. If a larger temperature change

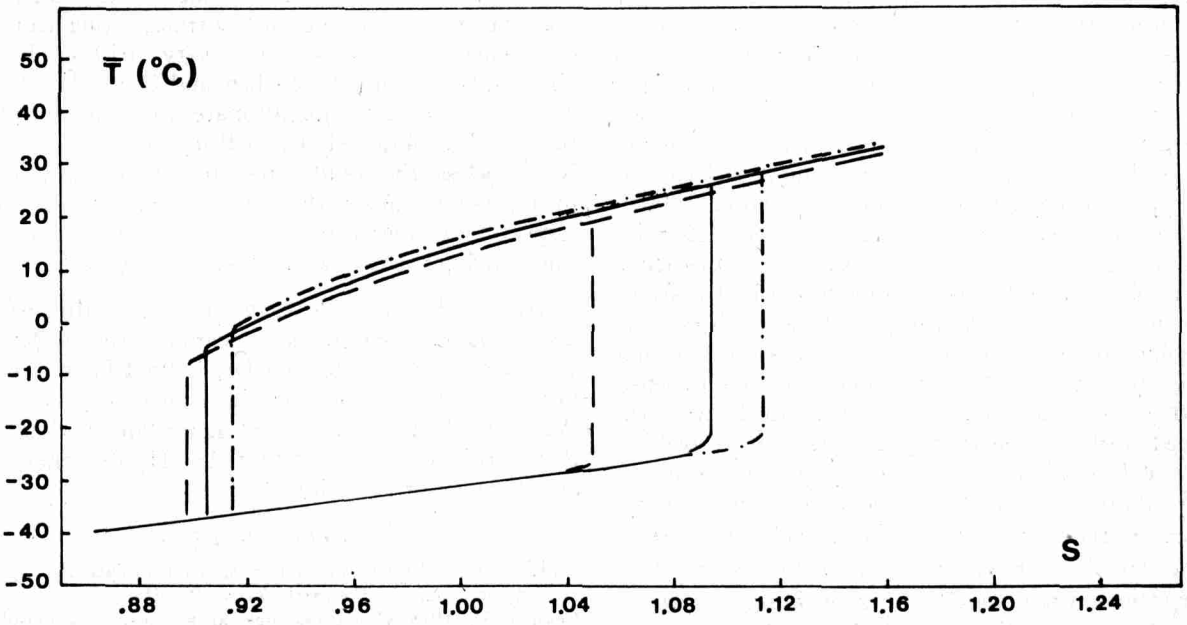

FIG. 11. Solution diagram for three diffusivities: $D=0.4$ (dashed line), $D=0.7$ (solid line), $D=1.0$ (dot-dashed line) W (m^2 °C)$^{-1}$. The solid line corresponds to the standard case.

were needed, as is the case with the weaker T,I coupling in previous models, the albedo-feedback mechanism dominates and the climate is more sensitive to change in S.

As stated before the diffusion of energy plays a minor role in our model; it neutralizes local energy deficits without having a principal influence on the characteristics of the model. Connected with the large value of b is the comparatively small variation of the temperature difference between pole and equator with S (see Fig. 9). In models in which the T,I coupling is weaker the diffusion term becomes more important so the pole-equator temperature difference may be expected to vary considerably with S. In many models this appears to be the case. It is interesting to compare these characteristics with some results of Gal-Chen and Schneider (1976). According to their Fig. 4 the pole-equator temperature difference decreases with increasing solar input if ice-albedo, temperature feedback is incorporated. If this feedback is omitted the reverse takes place. Since we found that a stronger T,I coupling suppresses the albedo feedback (of course this is only one way of interpretation), it is consistent with the results of Gal-Chen and Schneider that in our model the temperature gradient responds rather slightly to changes in S. This property is also reflected by the fact that within the range of interest, the effect of a change in S is almost completely equivalent to that of the same proportional change in the emissivity for the outgoing radiation, but with opposite sign.

We now turn to a discussion of the reliability of our results. Our model suggests that the present climate is rather stable and that we were *not* close to an icy disaster during the last ice age. This is a reassuring result but at the same time one should realize the shortcomings of the model used, the most important one probably being ignoring cloudiness variability. However, we feel that the results presented here have value for several reasons. The major one is the fact that the empirical input is based on a complete collection of satellite observations. Satellite measurements are the only way to determine *directly* the radiation balance at the top of the atmosphere, so they undoubtedly provide the best material to construct parameterizations of the albedo and outgoing radiation. Fig. 1b clearly shows that a simple parameterization of the infrared emission makes sense. Furthermore, the simulation of the albedo was performed without consistency factors and a realistic value of D was found. These facts give confidence.

In addition, it should be mentioned that, for our values of the various parameters, the mathematical properties of the model reflect a well-posed problem. Integrations from widely differing initial states all showed an uncomplicated evolution to the asymptotic equilibrium solution. Convergence was fairly rapid: in most cases 20 steps were sufficient to obtain an accuracy of 10^{-3} °C at every grid point and often only 10 steps or so were required. Altogether, the model appeared to be a highly damped system with rather definite characteristics, namely, the two-branch structure appearing for a wide range of empirical constants.

Another point that favors the plausibility of the results presented here is the occurrence of many glacial periods that apparently did not initiate a completely ice-covered earth. If the critical edge of the ice sheet (i.e., the latitude where evolution to the deep freeze starts spontaneously) were about 50° as reported by Budyko and others, we clearly have been very lucky. It seems more likely that the critical latitude is closer to the equator. In the Northern Hemisphere we found a critical latitude of 37° for the boundary of the more-than-50% ice cover whereas the corresponding latitude in the Southern Hemisphere is 50° (!).

Finally, we note in accordance to previous studies (e.g., Held and Suarez, 1974) that our EBM is not capable of supporting the ice-age theory of Milankovitch. Runs with different obliquities of the earth produced maximum temperature differences of only 1°C.

Summarizing, we conclude that satellite observations suggest that the characteristics of the present climate are dominated to a large extent by the coupling between temperature, planetary albedo and infrared emission, whereas the energy-transporting mechanism plays a minor role. These facts indicate that a possible influence of the general circulation on the thermal regime will operate via the coupling between the flow pattern and the distribution of clouds and water vapor (in close relation to the lapse rate) and much less via changes in the energy-transporting capacity of circulation systems. Since very little is known about this coupling (Gal-Chen and Schneider, 1976), at the present time an ultimate value judgment of the results obtained by EBM's is not possible. Nevertheless, the results presented in this paper point to a present climate that is much more stable with respect to temperature perturbations and changes in the solar input than has been assumed so far.

Acknowledgments. We thank Dr. S. J. Bijlsma for his valuable suggestions concerning the numerical treatment of the model and Dr. J. Reiff for the useful discussions we had during the course of this study. We also thank various colleagues for reading the manuscript, in particular Prof. Dr. H. Tennekes, who also gave editorial advice.

REFERENCES

Budyko, M. I., 1969: The effect of solar radiation variations on the climate of the earth. *Tellus*, **21**, 611–619.

Cess, R. D., 1976: Climate change: an appraisal of atmospheric feedback mechanisms employing zonal climatology. *J. Atmos. Sci.*, **33**, 1831–1843.

Chýlek, P. C., and J. A. Coakley, 1975: Analytical analysis of a Budyko-type climate model. *J. Atmos. Sci.*, **32**, 675–679.

CLIMAP, 1976: The surface of the ice-age earth. *Science*, **191**, 1131–1137.

Ellis, J. S., and T. H. Vonder Haar, 1976: Zonal average earth radiation budget measurements from satellites for climate studies. Atmos. Sci. Pap. No. 240, Colorado State University, 46 pp.

Faegre, A., 1972: An intransitive model of the earth-atmosphere-ocean system. *J. Appl. Meteor.*, **11**, 4–6.

Frederiksen, J. S., 1976: Nonlinear albedo-temperature coupling in climate models. *J. Atmos. Sci.*, **33**, 2267–2272.

Gal-Chen, T., and S. H. Schneider, 1976: Energy balance climate modeling: comparison of radiative and dynamic feedback mechanisms. *Tellus*, **28**, 108–121.

Gates, W. L., 1976: The numerical simulation of the ice-age climate with a global general circulation model. *J. Atmos. Sci.*, **33**, 1844–1873.

Ghil, M., 1976: Climate stability for a Sellers-type model. *J. Atmos. Sci.*, **33**, 3–20.

Hantel, M., 1974: Polar boundary conditions in zonally averaged global climate models. *J. Appl. Meteor.*, **13**, 752–759.

Held, I. M., and M. J. Suarez, 1974: Simple albedo feedback models of the icecaps. *Tellus*, **26**, 613–629.

Lamb, H. H., 1972: *Climate, Present, Past and Future*, Vol. 1. Methuen & Co. Ltd., 613 pp.

Lian, M. S., and R. D. Cess, 1977: Energy balance climate models: A reappraisal of ice-albedo feedback. *J. Atmos. Sci.*, **34**, 1058–1062.

Manabe, S., and T. B. Terpstra, 1974: The effect of mountains on the general circulation of the atmosphere as identified by numerical experiments. *J. Atmos. Sci.*, **31**, 3–42.

North, G. R., 1975a: Theory of energy-balance climate models. *J. Atmos. Sci.*, **32**, 2033–2043.

——, 1975b: Analytical solution to a simple climate model with diffusive heat transport. *J. Atmos. Sci.*, **32**, 1301–1307.

Oort, A. H., and T. H. Vonder Haar, 1976: On the observed annual cycle in the ocean-atmosphere heat balance over the Northern Hemisphere. *J. Phys. Oceanogr.*, **6**, 781–800.

Raschke, E., T. H. Vonder Haar, W. R. Bandeen and M. Pasternak, 1973: The annual radiation balance of the earth-atmosphere system during 1969–70 from Nimbus 3 measurements. *J. Atmos. Sci.*, **30**, 341–364.

Schneider, S. H., and T. Gal-Chen, 1973: Numerical experiments in climate stability. *J. Geophys. Res.*, **78**, 6182–6194.

Sellers, W. D., 1965: *Physical Climatology*. The University of Chicago Press, 272 pp.

——, 1969: A global climatic model based on the energy balance of the earth-atmosphere system. *J. Appl. Meteor.*, **8**, 392–400.

——, 1976: A two-dimensional global climate model. *Mon. Wea. Rev.*, **104**, 233–248.

Su, C. H., and D. Y. Hsieh, 1976: Stability of the Budyko-climate model. *J. Atmos. Sci.*, **33**, 2273–2275.

Temkin, R. L., and F. M. Snell, 1976: An annual zonally averaged hemispherical climate model with diffusive cloudiness feedback. *J. Atmos. Sci.*, **33**, 1671–1685.